JOURNAL OF MATERIALS SCIENCE: MATERIALS IN MEDICINE 3 (1992) 28–32

Scanning tunnelling microscopy and tunnelling spectroscopy of titanium before and after *in vitro* immersion

P. D. BIANCO, P. DUCHEYNE, D. BONNELL*
*Department of Bioengineering and *Department of Materials Science and Engineering, University of Pennsylvania, Philadelphia, PA 19104, USA*

In an effort to understand the *in vivo* interactions of titanium and its alloys with a biological environment, surface science methods have been used on specimens retrieved from *in vitro* and *in vivo* experiments. A relatively new technique that has the potential to further our knowledge of the oxide-solution interface is scanning tunneling microscopy (STM) and scanning tunneling spectroscopy (TS). This work documents the use of STM/TS in the study of titanium thin films before and after immersion in an *in vitro* solution. Titanium thin films were fabricated using a procedure which produced an oxide that had minimal contaminants. Half of the thin films were immersed in an electrolyte. STM/TS was performed immediately after the immersion period. Constant current images were obtained. Current–voltage characteristics were recorded at regions of interest. The topography of the nonimmersed films revealed that the surface was qualitatively the same as other sputter deposited metal films. I–V curves showed little spatial variation. The topography of the immersed film showed little change from the nonimmersed ones. However, significant spatial variation of the local electronic structure was noted. This indicates that titanium surface-fluid interactions do not occur uniformly on the film.

1. Introduction

Titanium and its alloys have been used with considerable clinical success for a variety of medical and dental applications. One factor is invariably invoked to explain the success of titanium-based implants: a favourable local tissue response [1, 2]. Since the interactions between a biomaterial and the surrounding tissues occur on a molecular scale within a small interfacial region, the importance of a detailed knowledge of the surface properties of the material is obvious.

Auger electron spectroscopy (AES) and X-ray photoelectron spectroscopy (XPS or ESCA) are two frequently used techniques for determining surface properties of titanium-based implants [3–7]. AES studies of retrieved titanium implants were performed by Sundgren and associates [4]. After an implantation period ranging from 0.5 to 3 years, they found an increase in oxide thickness as well as the incorporation of calcium and phosphorous (in the form of phosphates) into the oxide. XPS analysis of titanium and various alloys of titanium after immersion in NaCl and $FeCl_3$ solutions also showed oxide growth and incorporation of solution components into the oxide [5]. There are two main limitations to these and similar studies. Firstly, since the environment is complex and varies with time, interpreting the findings is difficult. Secondly, the surfaces are not often controlled. Contaminants such as carbon, which are invariably present in such studies, affect the interfacial reactions. Furthermore, variations in oxide thickness also influence the kinetics of these reactions. In short, if no measures are taken to ensure that a reproducible surface is present, sample to sample variation hinders the ability to gain insight into actual phenomena and mechanisms.

It was with these considerations in mind that Healy and Ducheyne [6, 7] conducted a dual AES and XPS analysis of titanium films. Titanium films could be reproducibly made with minimal contamination. They were characterized both before and after immersion in three *in vitro* modelling solutions. An increase in oxide thickness as well as adsorption of non-elemental phosphorous was observed. The same authors also utilized the sensitivity of XPS in detecting different chemical states to conduct a detailed characterization of hydroxylation of the surface after immersion. Before immersion, two types of hydroxyl groups (acidic and basic) were distinguished on the oxide surface. After immersion, there was an increase in OH groups detected.

Scanning tunnelling microscopy (STM) and tunnelling spectroscopy (TS) can provide additional information on the reactions occurring on the surface [8, 9]. STM provides atomic or near atomic resolution of the topography of the surface while TS yields

0022–2461/92 $03.00 + .12

TABLE I Surface characteristics (non-immersed film)

Trait	Method	Results	Reference
Elemental composition	AES and XPS	Ti, O, and C	6 and 7
Oxide thickness	Angle resolved XPS Ar sputtering and AES	~ 30 Å	7
Oxide stoichiometry	AES and XPS	TiO_2	7
Surface texture	STM	wavy	this study
Crystal structure	TEM	polycrystalline orthorhombic	unpublished data

electronic information that is directly related to the surface density of states. With the topographic mapping and the local electronic structure measurements, it is possible to determine spatial variation in the surface density of states. Ultimately, this can be related to the binding of various moieties at different locations.

It was with these goals in mind that the work presented in this short communication was initiated. The data reported here compliment the AES and XPS studies of titanium films [6, 7] with STM and TS analysis and compare for the first time both the topography and local electronic structure before and after immersion in an *in vitro* modelling solution.

2. Materials and methods

Both the specimens and the *in vitro* modelling solution were identical to the ones used for the previous AES and XPS work [6, 7]. The surface characteristics are summarized in Table I. In short, two titanium films were made by radio frequency (RF) sputter coating titanium onto silicon wafers (Ziti Inc., Los Gatos, CA, USA) with a (1 0 0) orientation. The silicon wafers had been treated following the cleaning procedures of the semiconductor industry [10]. Both the titanium target (Materials Research Corporation, Orangeburg, NY, USA) and the silicon wafers were sputter etched in the vacuum chamber for 5 min to remove their oxides. The titanium was then sputter deposited for 50 min at an approximate rate of 20 nm min^{-1}. The films were removed from the vacuum chamber and placed in an acid pickling solution composed of 8.33% (v) HNO_3 and 0.075% HF to remove the native oxide. The samples were immediately dried and allowed to stay in an oxygen chamber under an overpressure of O_2 for 24 h. The samples were passivated according to ASTM procedure [11] and ethylene oxide sterilized. One sample was immersed at once while the other was immediately inserted into the STM/TS vacuum chamber for analysis.

The *in vitro* modelling solution used was a modified Hank's balanced salt solution (HBSS) with 1.5 mM ethylenediaminetetraacetic acid (EDTA). The immersed specimens were placed in an incubator maintained at 37 °C with an atmosphere of 5% CO_2 and 21% O_2. The immersion lasted ~ 850 h. This time period was selected since previous work indicated that the adsorption of phosphate groups is well underway by this time [6]. After immersion, the sample was washed under flowing deionized H_2O for 5 min and dried with Argon gas. It was immediately transferred to the vacuum chamber for STM/TS analysis.

A commercial STM (WA Technology, Cambridge, UK) was used. All sample analysis was performed in UHV with a pressure less than 3×10^{-9} torr (4×10^{-7} Pa). Images were acquired in constant current mode. Subsequent to imaging, specific features were identified and the tip was moved to these features for spectroscopic analysis. The spectroscopy was performed by locking the tip at a fixed distance from the sample, ramping the voltage, and measuring the resulting current. After the acquisition of the I–V data at all desired spatial positions, the same area was imaged again to ensure that tip drift was minimal. Each sample (non-immersed and immersed) was imaged at over 20 different regions. Several different tip materials including gold, tungsten, and platinum were tried. To date, the best images and the most repeatable I–V curves have been obtained with gold tips. Tunnelling behaviour in vacuum and at atmospheric pressures was compared. In addition, *in situ* Auger analysis was performed to determine surface chemical composition.

Data processing for the imaging consisted of a high pass filter to remove noise. The I–V curves were smoothed, differentiated, and normalized to yield the dynamic to static conductance ratio, $[(dI/dV)/(I/V)]$, against V. These data have been shown to be related to the surface density of states [9].

3. Results

The topography of the non-immersed film is illustrated in Fig. 1. In both images, the intensity corresponds to vertical height with lighter shades indicating topographic peaks. Full-scale black to white is 35 Å. The topographic structure of this surface displays hilly features varying laterally in size from 1 nm to 0.1 μm and vertically from 1 nm to 10 nm. Similar results, however, with much lower resolution have been previously published [12]. The topography of the larger area shown in Fig. 2 exhibits a structure comparable with that shown in Fig. 1. Spatially localized electronic spectroscopy was performed on several locations widely apart on this surface. Representative spectra acquired at the locations a, b, and c indicated in Fig. 2 are presented in Fig. 3. Although spectroscopic data were acquired at four sample-tip separations at each location, the spectra shown in Fig. 3 were acquired at the same sample-tip separation. The value of the energy interval where the current is below the detection limit can be considered a measure of the apparent

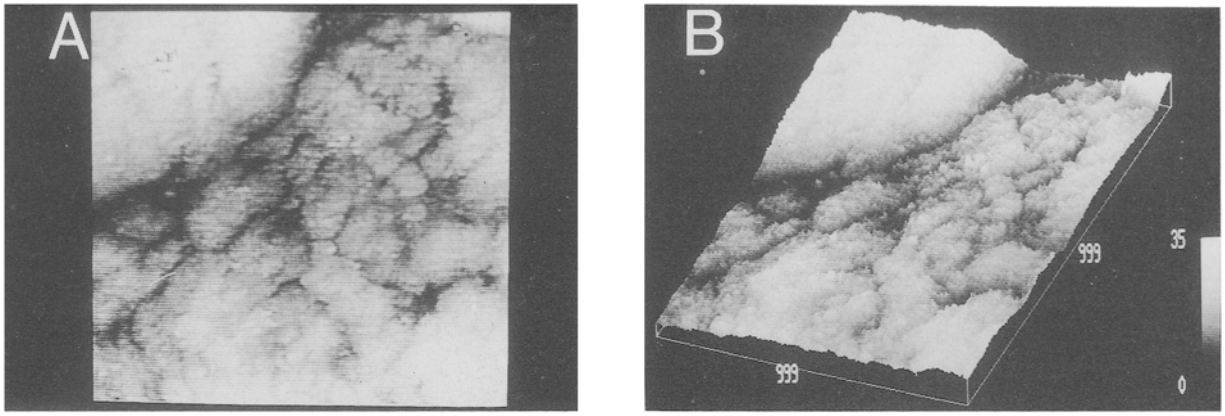

Figure 1 The grey scale (A) and three-dimensional (B) representation of the non-immersed film. This constant current image was acquired with a bias of 2.25 V and a tunnelling current of 0.25 nA. The dimensions are in ångströms.

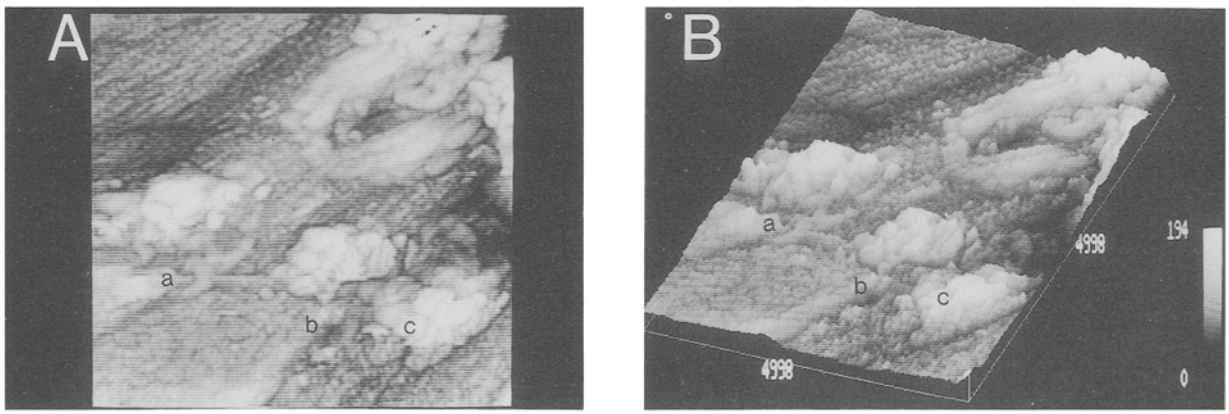

Figure 2 The grey scale (A) and three-dimensional (B) images of another region of the non-immersed film. The letters a, b, and c correspond to points where spectroscopy was performed. The imaging parameters were 2.25 V and 0.25 nA. Dimensions are in ångströms.

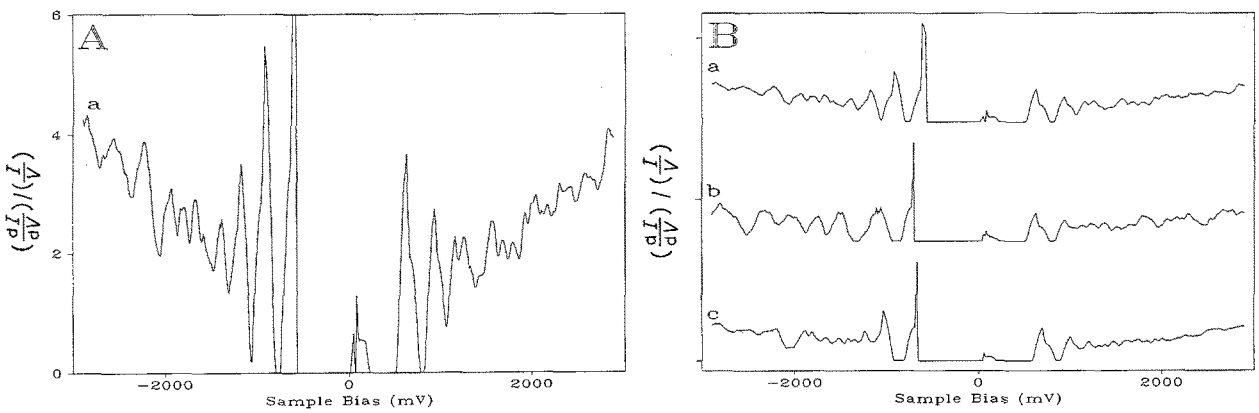

Figure 3 The dynamic/static conductance ratio vs voltage for location a (A) and for all three locations (B) in Fig. 2. Sample/tip separation was fixed with a bias of 1.5 V and a tunnelling current of 0.25 nA. The plots were made from 512 points and represent the average of 16 curves.

surface band gap between valence and conduction bands. Note that this quantity does not change as a function of position for the non-immersed surface. Additionally, the voltage position of the peaks are consistent for all three plots. These findings indicate that before immersion, there is a relatively uniform electronic structure. The Auger electron spectra show the presence of oxygen, titanium, and to a limited extent, carbon.

The grey scale and three-dimensional representations of the immersed film are shown respectively in Fig, 4A and 4B. The area is about 1000 Å × 1000 Å and full-scale black to white is 41 Å. Comparing these images to Fig. 1A and 1B, it is evident that there is no apparent change in topography as a result of immersion. Many other images not presented here also indicate that there is no perceptible effect of immersion on the surface geometry. Fig. 5 shows another grey scale image where at locations a, b, and c the tip was moved to obtain spectroscopic data. The $[(dI/dV)/(I/V)]$ against V plots for all three sites are shown in Fig. 6. In contrast to the spectroscopic data

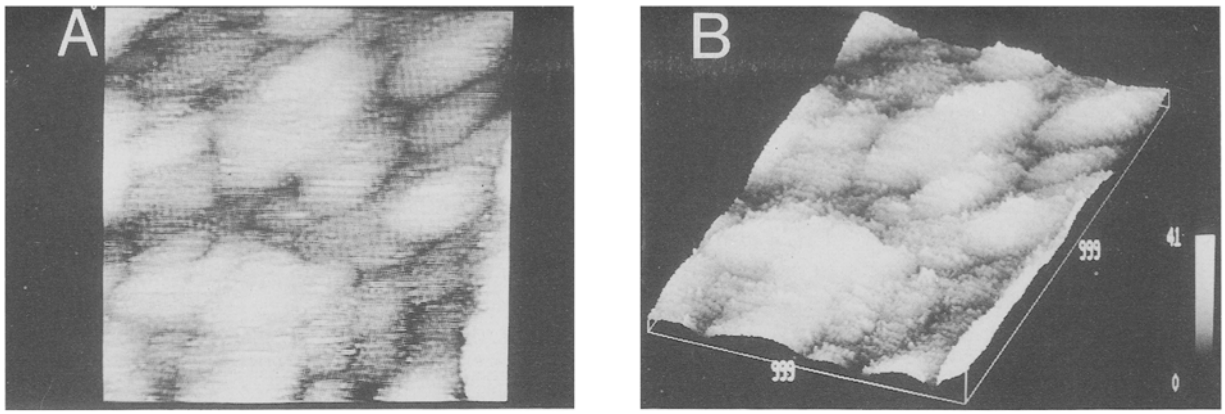

Figure 4 The grey scale (A) and three-dimensional (B) representation of the immersed film. Since the dimensions are in ångströms, this region is approximately the same size as Fig. 1. Imaging parameters were bias = 2.25 V and current = 0.25 nA.

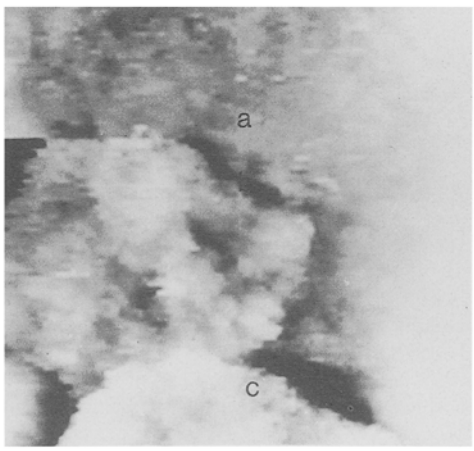

Figure 5 A grey scale image of another region of the immersed film. The letters a, b, and c mark the locations where spectroscopy was performed. The image size is ~ 790 Å × 790 Å. The white bar is 100 Å. The bias was 2 V and the tunnelling current was 9 nA.

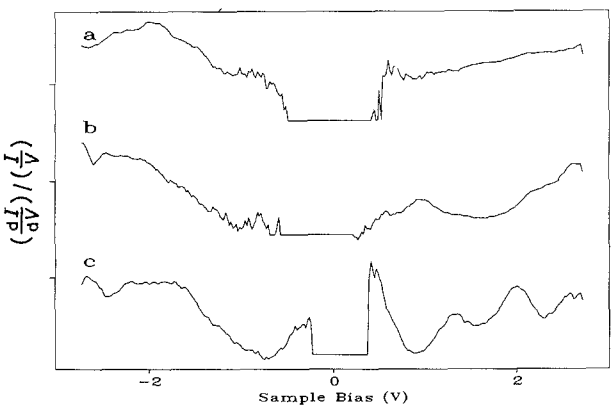

Figure 6 The dynamic/static conductance ratio vs voltage for locations a, b, and c of Fig. 5. Sample/tip separation was fixed with a bias voltage of 1.5 V and a tunnelling current of 1 nA. The plots were made from 512 points and represent the average of 10 curves.

for the non-immersed film (Fig. 3B), there is definitely spatial variation in local electronic properties evident on this surface. Specifically, the voltage positions of the peaks and the size of the interval where the conductance is not measurable around 0 V are different for each plot. This demonstrates that after immersion there is a non-uniform electronic structure. Auger electron spectra from the immersed film again show the presence of oxygen, titanium, and carbon. In addition, there is a P doublet indicating the presence of non-elemental phosphorous.

4. Discussion

The STM images presented here show, with a resolution not possible with SEM, that there is no apparent effect of immersion on the surface topography of titanium films. It is surprising that the surface has a hilly appearance. The TS spectra illustrate that before immersion a relatively uniform electronic structure is present. After immersion, there is spatial variation evident.

The hilly topography is attributable to the RF sputter deposition since other sputter-deposited metals have shown a similar surface aspect. As the oxide thickness is estimated to be 3 nm [7], given the much larger variations in height, the topography must represent the surface structure of the metal film. The oxide presumably followed the undulating nature of the underlying titanium. Our current interpretation is lent credence by recent TEM results. Oxide films 1000 Å thick on cold rolled anodically oxidized Ti-6Al-4V [13] showed features (which the authors call porosity) of the same order of magnitude as the hills in the STM images presented here. Since the surface preparation is so radically different from the one used here, the similarity of the structure is remarkable. After immersion, no meaningful change in morphology could be observed. Thus it would appear that the passive dissolution and reformation of the oxide are uniform and that the breaking off of oxide protuberances [14] did not contribute to the titanium release under the conditions of this experiment, in which, it must be remembered, there was no relative motion (wear) involved.

Whereas before immersion there was a uniform electronic structure, after immersion a spatial variation in electronic structure was detected. The variation found after immersion may be the result of replacement of hydroxyl groups found on the hydroxylated

oxide by phosphate groups [6]. To confirm this hypothesis, studies are now underway in which the oxide is either completely dehydroxylated or hydroxylated. Similar work in which the oxide is completely phosphorylated is envisioned.

The majority of the previous studies that used STM and/or TS to examine titanium have focused on the study of single crystals in vacuum [15] or air [16–18]. Although much can be learned from these model single crystals, work that uses systems modelling real implant materials [19, 20] is also needed. This experiment, where the effects of immersion on the topography and electronic structure on titanium films was studied with the resolution possible with STM/TS, represents a foundation on which future studies may build.

Acknowledgements

This research was supported in part by grants from the NSF (grant no. DMR 88-19885) and the N1I (grant no. 1-R01-AR-H0194). The authors express their gratitude to Dr Greg Rohrer for his invaluable help in operating the STM/TS and discussing the results.

References

1. T. ALBREKTSSON, P. I. BRANEMARK, H.-A. HANSSON, B. KASEMO, K. LARSSON, I. LUNDSTRÖM, D. McQUEEN and R. S. SKALAK, *Ann. Biomed. Engng* **11** (1983) 1.
2. D. F. WILLIAMS, in "Biocompatibility of clinical implant materials", edited by D. F. Williams (CRC Press Inc., Boca Raton, 1981) p. 9.
3. B. KASEMO and J. LAUSMAA, in "Surface characterization of biomaterials", edited by B. D. Ratner (Elsevier Science Publishers B.V., Amsterdam, 1988) p. 1.
4. J.-E. SUNDGREN, P. BODÖ and I. LUNDSTRÖM, *J. Coll. Inter. Sci.* **110** (1986) 9.
5. P.-A. MAEUSLI, P. R. BLOCH, V. GERET and S. G. STEINEMANN, in "Biological and biomechanical performance of biomaterials", edited by P. Christel, A. Meunier and A. J. C. Lee (Elsevier Science Publishers B.V., Amsterdam, 1986) p. 57.
6. K. E. HEALY and P. DUCHEYNE, *Biomaterials*, submitted.
7. K. E. HEALY and P. DUCHEYNE, *J. Coll. Inter. Sci.*, submitted.
8. P. K. HANSMA and J. TERSOFF, *J. Appl. Phys.* **61** (1987) R1.
9. R. J. HAMERS, *Ann. Rev. Phys. Chem.* **40** (1989) 531.
10. W. KERN and D. A. PUOTINEN, *RCA Rev.* **31** (1970) 187.
11. Standard recommended practice for surface preparation and marking of metallic surgical implants, *ASTM Standard F86*, ASTM, Philadelphia (1976).
12. A. M. BARÓ, N. GARCIA, R. MIRANDA, L. VÁZQUEZ, C. APARICIO, J. OLIVÉ and J. LAUSMAA, *Biomaterials* **7** (1986) 463.
13. M. ASK, U. ROLANDER, J. LAUSMAA and B. KASEMO, *J. Mater. Res.* **5** (1990) 1662.
14. R. J. SOLAR, S. R. POLLACK and E. KOROSTOFF, *J. Biomed. Mater. Res.* **13** (1979) 217.
15. G. S. ROHRER, V. E. HENRICH and D. A. BONNELL, *Science* **250** (1990) 1239.
16. F.-R. F. FAN and A. J. BARD, *Phys. Chem.* **94** (1990) 3761.
17. S. E. GILBERT and J. H. KENNEDY, *Surf. Sci. Lett.* **225** (1990) L1.
18. K. SAKAMAKI, S. MATSUNAGA, K. ITOH, A. FUJISHIMA and Y. GOHSHI, *ibid.* **219** (1989) L531.
19. P. D. BIANCO, P. DUCHEYNE, D. BONNELL and G. ROHRER, in Transactions of the Society for Biomaterials, Charleston, May 1990, p. 64.
20. M. JOBIN, R. EMCH, F. ZENHAUSERN and P. DESCOUTS, in Fifth International Conference on Scanning Tunnelling Microscopy/Spectroscopy, Baltimore, July 1990, p. 241.

Received 5 November 1990
and accepted 11 January 1991